

THE IMPLEMENTATION AND EFFECTIVENESS OF AIR INFILTRATION
STANDARDS IN BUILDINGS

5th AIC Conference, October 1-4 1984, Reno, Nevada, USA

PAPER 20

VERIFICATION OF CALCULATION MODELS OF AIR INFILTRATION USING
THREE TYPES OF TEST HOUSES

Hiroshi YOSHINO¹, Fusao HASEGAWA¹ AND Yasuo UTSUMI²

¹Department of Architecture,
Faculty of Engineering,
Tohoku University, Sendai 980
Japan

²Department of Architecture,
Miyagi National College of Technology,
Natori-shi, Miyagi Prefecture, 981-12
Japan

SYNOPSIS

In order to verify the calculation models of air infiltration using three wooden test houses which have the same type of construction but have different leakage distributions, airtightness of building components of these three houses were measured by means of the fan pressurization method, and then air infiltration was measured twenty-two times by CO₂ concentration decay technique. Some of the leaks were sealed so that total leakage of each of the three houses was equal, but the leakage distribution was different between House A and House B, and the amount of total leakage of House C was twice that of House A and of House B.

Secondly, air infiltration was calculated by means of the LBL model and the BRE model. The values as calculated by the LBL model were unexpectedly two to three times the values of measurement. The values as calculated by the BRE model were in the range of one to two times the values of measurement.

Thirdly, calculation by means of the JCV model widely used in Japan was done under the assumption of there being five types of leakage distribution in order to clarify the effect of leakage distribution on the accuracy of estimation. With the JCV model the internal pressure and the air infiltration are calculated by the Newton Raphson method using an equation in which the total infiltration is zero. Before this calculation, the pressure difference due to the combination of the wind and stack effects is introduced into the leakage equation for each leak.

As a result, the best estimation is yielded by the uniform distribution as opposed to the other distributions. So, it can be said that the assumption of uniform distribution of leakage can be accepted in the case of a house which is not so much airtight.

LIST OF SYMBOLS

- n' : Predicted value of air infiltration ratio, 1/h
 n : Measured value of air infiltration ratio, 1/h
or flow exponent used in leakage air flow equation
 v : Wind velocity, m/s
 ΔT : Indoor-outdoor temperature difference, °C
 T : Indoor temperature, °C
 g : Gravity acceleration, m/s²
 ρ_r : Indoor air density, kg/m³
 ρ_o : Outdoor air density, kg/m³
 Δp : Pressure difference across a leakage, Pa
 Δp_o : Indoor-outdoor base pressure difference, Pa
 p_r : Indoor pressure at the floor level, Pa
 A_o, A_c, A_f : Equivalent leakage area of the envelope, the ceiling, and the floor, respectively, cm²
 A_i : Wall area of i , m²
 H : Ceiling height, m
 h : Height from the floor level, m
 Q : Air infiltration rate or leakage flow rate, m³/h
 Q_o : Leakage flow rate for $\Delta p = \Delta p_o$, m³/h
 Q_i, Q_c, Q_f : Leakage flow rates through wall i , ceiling and floor, respectively, m³/h
 Q_w : Air infiltration rate due to the wind effect, m³/h
 Q_s : Air infiltration rate due to the stack effect, m³/h
 C_i : Wind pressure coefficient on wall i
 C_r : Indoor pressure coefficient
 a_i, a_c, a_f : Wind pressure coefficients of wall i , ceiling and floor as based on indoor pressure, respectively
 $A_r = T \cdot g \cdot H / ((t+273) \cdot v^2)$
 $Z = h/H$
 $B = 2 \cdot A_r$
 ϕ : Wind direction
 a, b, c : Regression coefficients

1. INTRODUCTION

It is very important to precisely predict the air infiltration of a house for the purpose of estimating the heating load and the indoor air quality. As more attention is being paid to thermal insulation and airtightness of residential buildings from the viewpoint of energy conservation, this subject is becoming more and more important. One reason is that the ratio of heating loss due to air infiltration increases with thermal insulating of a house, in comparison to the ratio of heat loss through the walls. Another reason is that the indoor air is easily polluted with various contaminants when a house is made airtight; further study of this contamination is becoming necessary due to the above mentioned improvement.

However, the method for precisely predicting air infiltration has not been developed because of the following reasons:

a) Air leakage of a building can be found not only around doors and windows but also at the following parts of the building:

- 1) holes for wall pipes,
- 2) electric outlets,
- 3) joints between the wall and the window frames,
- 4) interfaces between the ceiling and walls,
- 5) interfaces between the floor and walls,
- 6) wall surfaces and ceiling surfaces themselves.

These leakages cannot be identified at the planning stage.

b) The airtightness of windows installed in walls is often different from the catalog data. This is affected by the quality of construction. The measured values are generally greater than those data listed in a catalog.

c) As there is little data on wind pressure coefficients, it is difficult to estimate the appropriate coefficient for each house.

d) Wind velocity and wind direction is always fluctuating. Evaluation of the effect of this fluctuation on air infiltration has not been possible up to now.

e) It is difficult to estimate air infiltration when window and doors are opened and closed.

Problems a) and b) mentioned above are dependent on the quality of construction; therefore, airtightness should be measured. Items c), d) and e) are major areas needing further research.

In this paper, as the first stage in the development of a method for predicting air infiltration, attention is focused on verification of air infiltration in single-room-calculation models. Wind pressure on the envelope and indoor-outdoor temperature differences were measured for three types of test

houses for which airtightness data had already been obtained.

Three prediction models, the LBL model¹, the BRE model² and the JCV model³ were evaluated. The JCV model, which is explained later, is the model widely used in Japan for calculation of ventilation.

Some of leaks of three test houses were sealed so that the total leakage of House A and of House B was equal, but the leakage distribution of House A and House B differed, and the total leakage of House C was twice that of House A and of House B.

2. MEASUREMENT OF AIRTIGHTNESS AND AIR INFILTRATION OF TEST HOUSES

2.1 Test houses and their surroundings

The photograph of the three test houses and their plan are shown in Fig.1 and Fig.2, respectively. Each of these wooden houses has a single room with windows in all four walls and also have attic space and crawl space except for House C which has no crawl space, because the wooden floor is constructed directly on the concrete slab which is directly on top of the ground. The attic space and the crawl space have ventilation inlets. Floor area is 23.7 m². Room air volume is 60 m³.

The test houses were constructed in the courtyard of a factory in Yamagata Prefecture. The surroundings of the houses are shown in Fig.3. The main factory building is northwest of the houses. On the southeast is an orchard. There is no obstacle blocking the wind from the south. Wind direction varied between ENE and ESE during the first year of measurement. During the measurement period in the second year, wind was from the east and also from other directions; however the measured data was only analysed with regard to wind from the east.

2.2 Airtightness of houses

2.2.1 Method for obtaining airtightness

After a duct with an attached fan was installed in the hole previously opened for the ventilation fan, airtightness of the houses was measured by means of the fan pressurization method. The range of indoor-outdoor pressure difference was 3 to 50 Pa. Pressure was measured by a capacitance manometer. Speed of flow at the center of the duct was measured using a thermistor anemometer, and airflow rate was estimated based on previously obtained data as to the relationship between the wind speed at the center and the airflow rate.

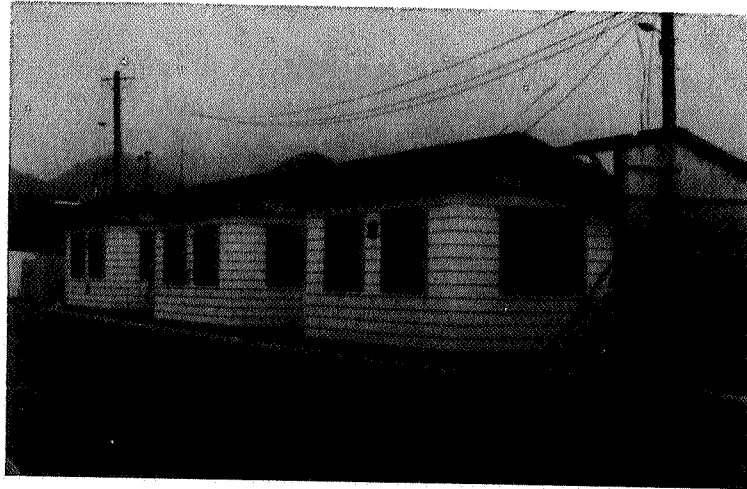


Fig.1 View of the test houses from the west

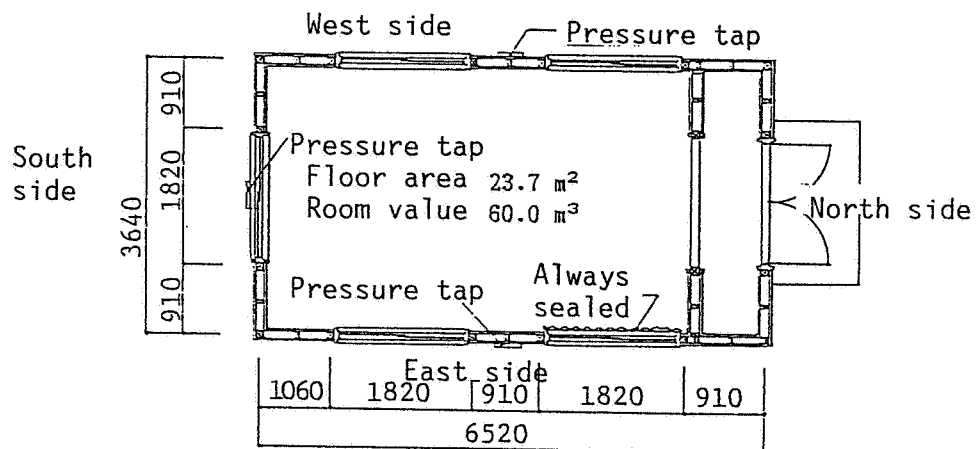


Fig.2 Plan of the test houses

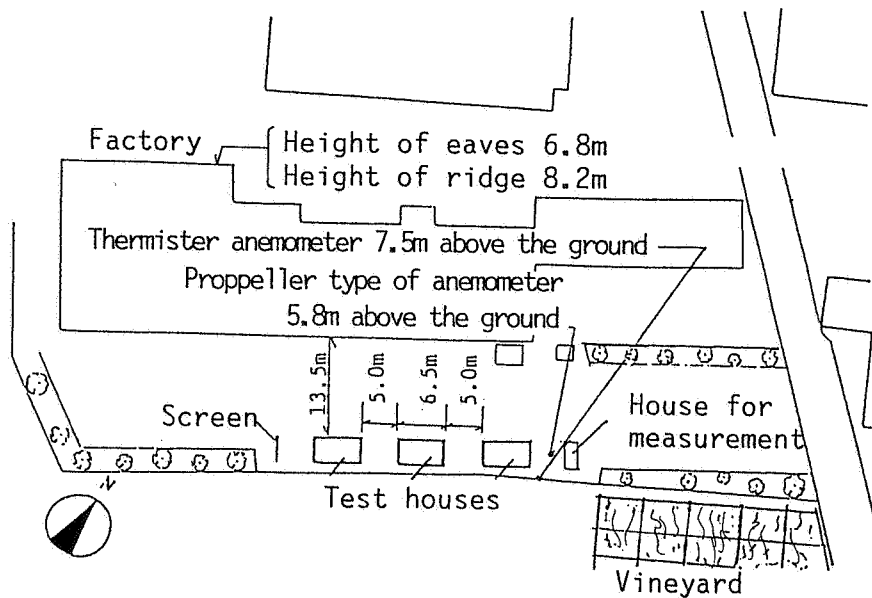


Fig.3 Site plan of the test houses

2.2.2 Measured results

The measured results of airtightness of the building elements are shown in Fig.4. If the relationship between the indoor-outdoor pressure difference, Δp , and the flow rate, Q , is shown by equation (1), the flow rate, Q_0 , for $\Delta p_0=10$ Pa and the flow component, n , of each leakage can be indicated as in Table 1.

$$Q = Q_0(\Delta p/\Delta p_0)^{1/n} \quad \text{-----}(1)$$

In House A, the interface between the floor and walls and the southern window were sealed with vinyl sheeting. In House B, the eastern window, the southern windows and the northern windows except for one of the northern windows were sealed. But in House C no leaks were sealed. The equivalent leakage area per floor area (specific leakage area) of a whole house can be calculated by

$$A_0 = 2.78 \sqrt{\rho/2} Q_0 \quad \text{-----}(2)$$

Specific leakage areas of House A, B and C are 7.6, 8.1 and 14.7 cm^2/m^2 , respectively. These values fall between Airtightness Rank 4 and 5 as shown in Ref.4. This means that the airtightness of the test houses is equivalent to that of popular prefabricated houses in Japan.

As a result of sealing some leaks, the total leakage of House A and House B was equal, but the leakage of the western window of House A and the interface between floor and walls of House B were comparatively great. The total leakage of House C was 1.9 and 1.8 times greater than that of House A and of House B, respectively. The western window of House C was especially leaky.

At the beginning of the second year, the airtightness of the three houses was tested by the fan pressurization method after the same leaks as had been sealed in the first year were once again sealed. The results are shown in the lower part of Table 1. Q_0 of House A in the second year was nearly equal to that of House A measured in the first year. However, the values of Q_0 of House B and House C were 19 % and 13% smaller, respectively, than the values obtained in the first year. These differences may be due to changes in outdoor temperature and humidity, changes of building material characteristics, differences in the method of sealing, etc. The average outdoor temperature and humidity during the period of measurement, including the 5 days before measurement, were 26.5°C and 80.4 % in the first year and 25.2°C and 61.8 % in the second year. The humidity in the first year was more than that in second year. If humidity affects airtightness, then a difference in airtightness of House A should have been observed between the first year and the second year, and also, Houses B and C should have been more airtight during the more humid first year. Therefore, the difference does not seem to be due to the effect of humidity. Other possible reasons were not investigated.

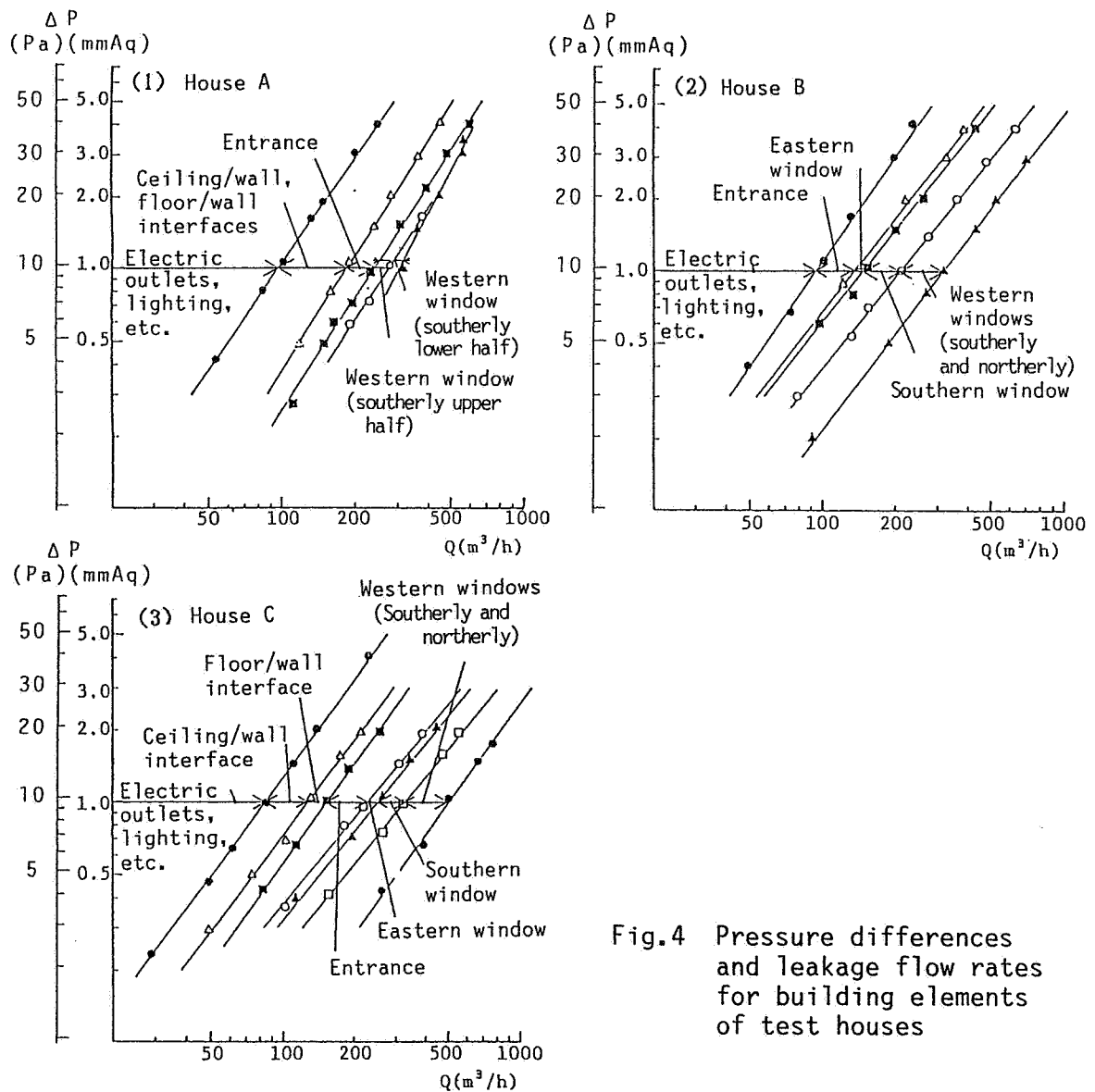


Fig.4 Pressure differences and leakage flow rates for building elements of test houses

Table 1 Effective leakage areas of building elements

	House A		House B		House C		
	Q _o (m ³ /h)	n	Q _o (m ³ /h)	n	Q _o (m ³ /h)	n	
Entrance	51.2	1.34 1)	52.6	1.21	74.6	1.09	
Eastern window	9.6	1.0(0.97)	—	—	24.4	1.08	
Southern window	—	—	—	—	74.2	1.29	
Western window	107.0	1.43	35.3	1.13	177.5	1.67	
Floor/wall interface	—	—	92.7	1.93	24.8	2.0(2.14)	
Other obscure leakages	94.9	1.5	99.6	1.57	① 43.6 2)	1.22	
					② 86.5	1.36	
Total	First year	262.7	1.31	280.2	1.47	505.6	1.36
	Second year	252.5	1.37	226.8	1.49	438.9	1.47

- 1) The values in parentheses were obtained by measurement. Because the flow component n varies between 1 and 2, $n=1$ when $n<1$, $n=2$ when $n>2$ in later calculation.
- 2) The values of ① and ② are for ceiling/wall interfaces and "other obscure leakages", respectively.

2.2.3 Height of the neutral level

After the indoor-outdoor temperature difference was stabilized at around 20°C by means of the method described later, the indoor-outdoor pressure difference at a point 2.1 m above the floor, was measured under calm outdoor conditions. In Houses A, B and C, the measured pressure differences were 0.9, 0.8 and 0.4 Pa, and the neutral levels were calculated to be 1.21, 1.30 and 1.69 m above the floor, respectively. The ceiling height was 2.42 m. The neutral level was nearly equal between House A and House B, while that of House C was slightly higher.

2.3 Measurement of air infiltration

2.3.1 Methods of measurement

Methods of measurement of air infiltration ratio, pressure, temperature, etc. is outlined in Table 2.

(1) Air infiltration ratio

The infiltration ratio was measured by the CO₂ concentration decay technique. While the air in the room was being circulated by two fans, the air at the center of the room was absorbed through rubber pipe into a CO₂ interferential concentration meter. The interval between measurements was 10 minutes for Houses A and B, and 5 minutes in the case of House C.

(2) Pressure and temperature

During the first year, the pressures were measured only on the building envelope of House A. On the basis of the pressure at the level of 2.1 m above the floor, the surface pressures on the four outer walls at the same level and the pressures in the attic and crawl spaces were measured by means of two pressure transducers which were switched every two minutes. During the second year, in order to find the pressure distribution among the three test houses, the surface pressure on the outer walls of House B and C were measured with the corresponding surface pressure of House A being used as a reference point.

Indoor temperatures were measured 1 m above floor level at the center of the room by a thermocouple and a multi digital recorder after ascertaining that there was no vertical temperature difference.

(3) Outdoor environment

Wind velocity was measured by a thermistor anemometer standing 7.5 m above ground level, and the wind direction was measured by the propeller type of the anemometer 5.8 m above ground level.

Table 2 Techniques for measurement of infiltration rates, etc.

	Measurement techniques	Instruments
Infiltration rates	CO ₂ concentration decay	CO ₂ interferometer
Indoor-outdoor pressure difference	Pressure are measured at the outsides of four walls, in the attic and in the crawl space, on the basis of the indoor pressure at a level 2.1m above the floor. (The surface pressure on the outer walls of Houses B and C were measured on the basis of wall surface pressure of House A corresponding to those of the other houses.)	Capacitance-type of pressure transducer
Room temperature	Measured at the center of each room 1.0m above the floor.	Thermo-couples and electric digital recorder
Air temperature	Measured in the screen	Thermo-couples
Wind speed and direction	Wind speed at a height of 7.5m and wind direction at a height of 5.5m.	Thermistor anemometer & propeller type of anemometer

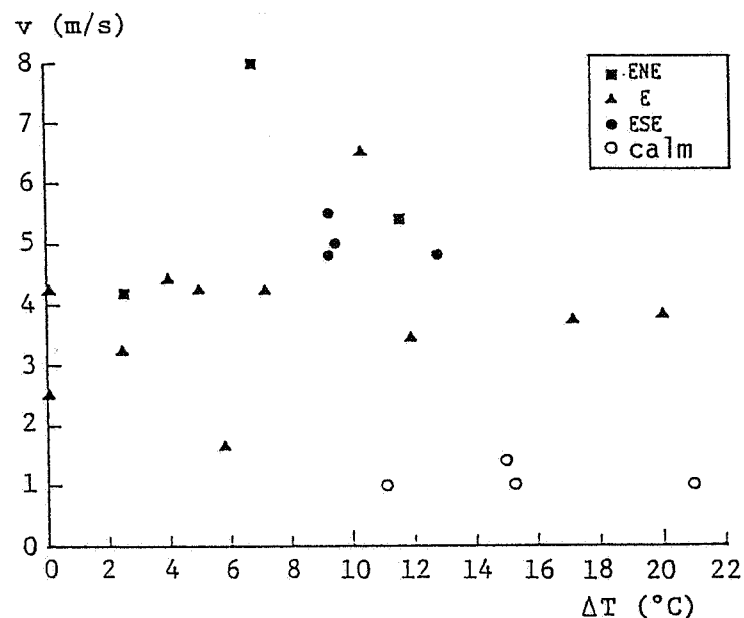


Fig.5 Experimental condition (Relationship between wind speed and indoor-outdoor temperature difference)

Outdoor temperature was measured by a thermocouple mounted in a screen.

2.3.2 Conditions of measurement

Indoor temperature was controlled in the range of $\pm 1^{\circ}\text{C}$ by heaters which automatically switched on and off. Relationship of the indoor-outdoor temperature difference and the wind speed is shown in Fig.5. Wind velocity was distributed between 0 and 8 m/s, and temperature difference was 0 to 21°C . Wind direction was ENE to ESE.

2.3.3 Measurement results

(1) Relationship of air infiltration ratio between three test houses

Table 3 shows the measured results. No.21 and No.22 were measured during the second year. The average infiltration ratios excluding No.6 of House A, B and C were 0.30, 0.31 and 0.76 1/h, respectively. The difference of leakage distribution between House A and House B had no influence on the infiltration ratio. While the leakage area of House C was twice that of both House A and House B, the infiltration ratio of House C was about 2.5 times that of House A and House B. This means that the infiltration ratio didn't rise in proportion to the increase of the total leakage.

Fig.6 shows the relationship of air infiltration between House A and House B or between House A and House C. The relationship varied according to the direction of wind. In the cases of Houses B and C, the air infiltration ratios were relatively great when the wind direction was ESE. When wind direction was ENE or E, these ratios were relatively small. This may be because Houses A and B prevented Houses B and C from exposure to wind from the E and ENE.

(2) Factors influencing air infiltration ratio

Fig.7 shows the relationship between the wind velocity and the infiltration ratio. The infiltration ratio rose with an increase in wind velocity. This tendency is especially evident in the case of House C. The infiltration ratio increased slightly when the indoor-outdoor temperature difference became greater under a constant wind velocity.

(3) Regression analysis of the relationship between infiltration ratio and factors affecting this ratio

Bahnfleth et al.⁵ show that the infiltration ratio, Q , can be expressed by a linear equation (3) which includes the indoor-outdoor temperature difference, T , and the wind velocity, v , as variables.

Table 3 Experimental results

Exp. No.	Wind direc.	Wind Speed (m/sec)	Outdoor temp. (°C)	Indoor temp. (°C)			Wind pressure coeff. (House A)						Measured infiltr. ratios (1/h)		
				House A	House B	House C	East	South	West	North	In ceiling	Below Floor	House A	House B	House C
1	ENE	8.0	23.8	30.3	30.8	30.7	0.16	-0.05	-0.10	0.02	0.08	0.02	0.57	0.50	1.25
2	E	6.5	21.1	31.4	31.0	32.0	0.19	-0.01	-0.06	0.10	0.06	0.02	0.49	0.50	1.16
3	ESE	4.8	27.3	40.4	39.9	39.9	0.25	-0.08	-0.13	-0.04	0.06	0.02	0.37	0.41	1.06
4	ESE	5.5	25.8	35.1	35.1	35.1	0.34	-0.08	-0.12	0.05	0.06	0.02	0.49	0.60	1.46
5	ESE	5.0	25.1	35.1	34.4	34.3	0.38	-0.12	-0.12	0.07	0.06	0.02	0.43	0.46	1.21
6	ESE	4.8	23.1	32.9	32.4	—	0.37	-0.04	-0.10	0.12	0.06	0.02	0.41	0.50	—
7	E	4.4	20.3	24.0	24.2	24.6	0.37	-0.14	-0.14	0.15	0.06	0.02	0.36	0.34	0.98
8	E	3.4	19.0	30.9	30.5	31.2	0.34	-0.24	-0.13	0.08	0.06	0.02	0.28	0.28	0.71
9	E	3.7	18.5	35.6	35.7	35.4	0.44	-0.12	-0.18	0.17	0.06	0.02	0.37	0.37	0.34
10	E	3.7	18.6	38.4	38.5	39.1	0.32	-0.15	-0.15	0.26	0.06	0.02	0.43	0.36	0.86
11	ENE	4.2	24.4	26.8	26.6	27.5	0.21	-0.06	-0.15	0.34	0.06	0.02	0.31	0.29	0.63
12	E	3.2	25.7	28.0	27.8	28.8	0.21	0.02	-0.19	0.25	0.06	0.02	0.13	0.20	0.45
13	ENE	5.4	24.7	35.7	36.8	36.5	0.20	-0.08	-0.16	0.32	0.06	0.02	0.50	0.45	1.05
14	E	4.2	21.2	26.0	26.1	26.5	0.23	-0.13	-0.16	0.34	0.06	0.02	0.38	0.30	0.86
15	E	4.2	20.6	28.1	27.5	27.9	0.23	-0.11	-0.18	0.31	0.06	0.02	0.39	0.30	0.89
16	0	1.0	19.6	31.0	30.2	31.0	0.0	0.0	0.0	0.0	0.0	0.0	0.09	0.13	0.27
17	0	1.0	18.8	33.9	34.6	33.9	0.0	0.0	0.0	0.0	0.0	0.0	0.10	0.20	0.31
18	0	1.4	20.7	35.9	36.0	35.3	0.0	0.0	0.0	0.0	0.0	0.0	0.11	0.17	0.32
19	E	1.6	19.3	25.4	24.9	25.0	0.25	0.00	-0.06	0.25	0.06	0.02	0.10	0.08	0.24
20	0	1.0	19.9	41.2	41.0	40.5	0.0	0.0	0.0	0.0	0.0	0.0	0.17	0.23	0.44
21	E	4.2	29.2	29.4	27.4	28.9	0.09	-0.08	-0.10	0.10	0.02	0.00	0.16	0.19	0.59
22	E	2.5	20.9	21.0	21.6	20.8	0.24	-0.03	-0.17	0.24	0.10	0.10	0.15	0.15	0.33
Average													0.31	0.32	0.76

No.1~No.20 were measured in the first year.

No.21 and No.22 were measured in the second year.

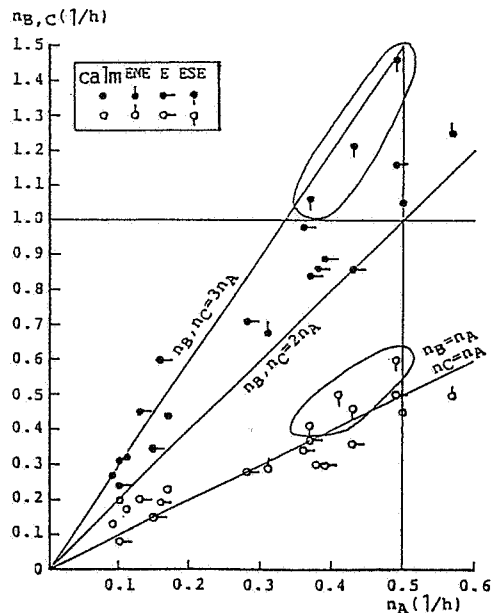


Fig.6 Comparison of infiltration ratios between Houses A, B and C

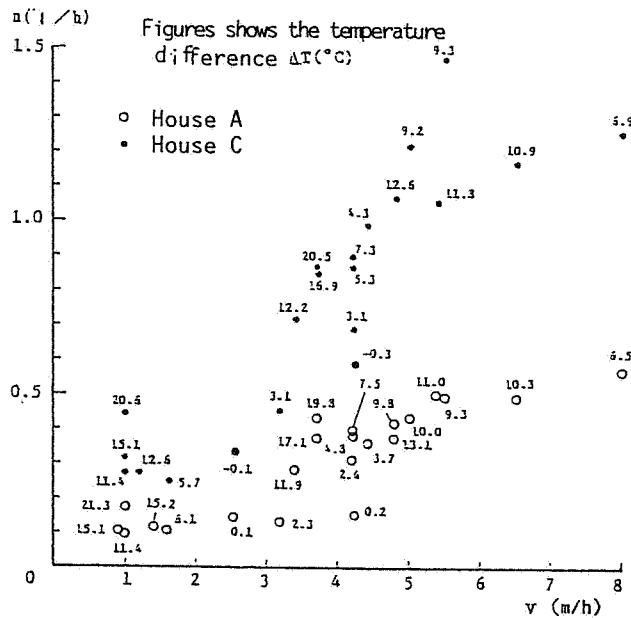


Fig.7 Measured infiltration ratios of Houses A and C

Table 4 Average wind pressure coefficient

Wind direc.	East	South	West	North
ENE	0.19	-0.06	-0.14	0.23
E	0.26	-0.09	-0.14	0.20
ESE	0.34	-0.08	-0.12	0.05

$$Q = a + b \Delta T + c v \quad \text{----- (3)}$$

On the basis of the measured results, the regression equations obtained which predict the infiltration ratio, n' , are:

$$\begin{aligned} \text{House A: } n' &= -0.0904 + 0.0087 \Delta T + 0.0831 v \\ \text{House B: } n' &= -0.0490 + 0.0096 \Delta T + 0.0729 v \\ \text{House C: } n' &= -0.0987 + 0.0162 \Delta T + 0.1873 v \end{aligned} \quad \text{----- (4)}$$

The correlation coefficients of the predicted value, n' , obtained by Eq.(4) and the measured value, n , are as high as 0.95, 0.92 and 0.93 in cases of Houses A, B and C, respectively. The partial regression coefficient of ΔT is remarkably smaller than that of v . In the case of C, the coefficients of ΔT and v are larger than those of Houses A and B, corresponding to the relatively high level of total leakage of House C.

2.4 Pressure distribution around the building envelope

Table 3 includes the wind pressure coefficient of House A based on wind velocity 7.5 m above ground level as obtained by Eq.(5). The stack effect due to indoor-outdoor temperature difference is not included.

$$C = (p_i - p_r)/(\rho v^2/2) \quad \text{----- (5)}$$

As the wind was mainly from the east, the pressure on the surface of the east wall was usually plus and that on the west wall was minus. Table 4 shows the mean wind pressure coefficient for each wind direction.

In the second year, the distribution of the wind pressure coefficients for Houses A, B and C were measured when the wind was from the east. Fig.8 shows the wind pressure coefficients of various points as based on the indoor pressure in House A. The values for the north wall of House B and C were smaller than that for House A due to wind being blocked by the adjacent test houses. This is related to the results shown in Fig.6 in that the infiltration ratio is rather small in the case of wind from the east.

The wind pressure coefficient of the wall surface 1 m above ground level is much smaller for the east and north walls and larger for the west wall, which is to be expected.

The wind pressure coefficient of Houses B and C used in Chapter 3 for the evaluation of the calculation model is the same value as that of House A for a wind direction of ESE. Coefficients in the case of wind from the E or ENE are also given as based on the pressure coefficient of House A in view of the difference as shown in Fig.8. The pressure difference between the upper and lower parts of the wall as measured for House A was taken into

consideration to calculate the mean pressure for each wall. The pressure coefficients of the attic space and the crawl space are given as the mean value of tests No.21 and No.22.

3. VERIFICATION OF CALCULATION MODELS

3.1 LBL model

3.1.1 Model

Air flow rate through leakage is assumed to be given by Eq.(6) in the range of $\Delta p=2$ to 10 Pa.

$$Q = A_o \sqrt{(\rho/2) \Delta p} \quad \text{----- (6)}$$

Based on the result of the pressurization test, the effective leakage area, A_o , is calculated for $\Delta p=4$ Pa. Air infiltration rates, Q_w and Q_s , which depend on the wind effect and the stack effect are respectively expressed by

$$Q_w = 3600 f_w A_o v \quad \text{----- (7)}$$

$$Q_s = 3600 f_s A_o \sqrt{gH\{\Delta T/(T+273)\}} \quad \text{----- (8)}$$

where

$$f_w = C'(1 - R)^{1/3} \quad \text{----- (9)}$$

$$f_s = 1/3 (1 + R/2) \{1 - X^2/(2 - R)^2\}^{3/2} \quad \text{----- (10)}$$

and

$$C' = 1/2 (\sqrt{|C_i - C_r|}) \quad \text{----- (11)}$$

$$R = (A_c + A_f)/A_o \quad \text{----- (12)}$$

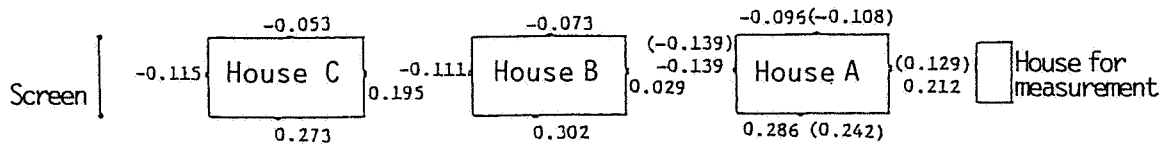
$$X = (A_c - A_f)/A_o \quad \text{----- (13)}$$

When the wind effect and the stack effect act simultaneously, these two effects can be combined as:

$$Q = \sqrt{Q_w^2 + Q_s^2} \quad \text{----- (14)}$$

These equations are based on the following assumptions:

- a) leakage is uniformly distributed on each wall, ceiling and floor;
- b) the air flow through leakage is turbulent;
- c) wind pressure coefficients of the ceiling and the floor are zero, and
- d) prevailing wind direction can not be ascertained.



Figures in the parentheses indicate the coefficients at the level of 1.0m above the ground East wind

Fig.8 Measured wind pressure coefficients of test houses (East wind)

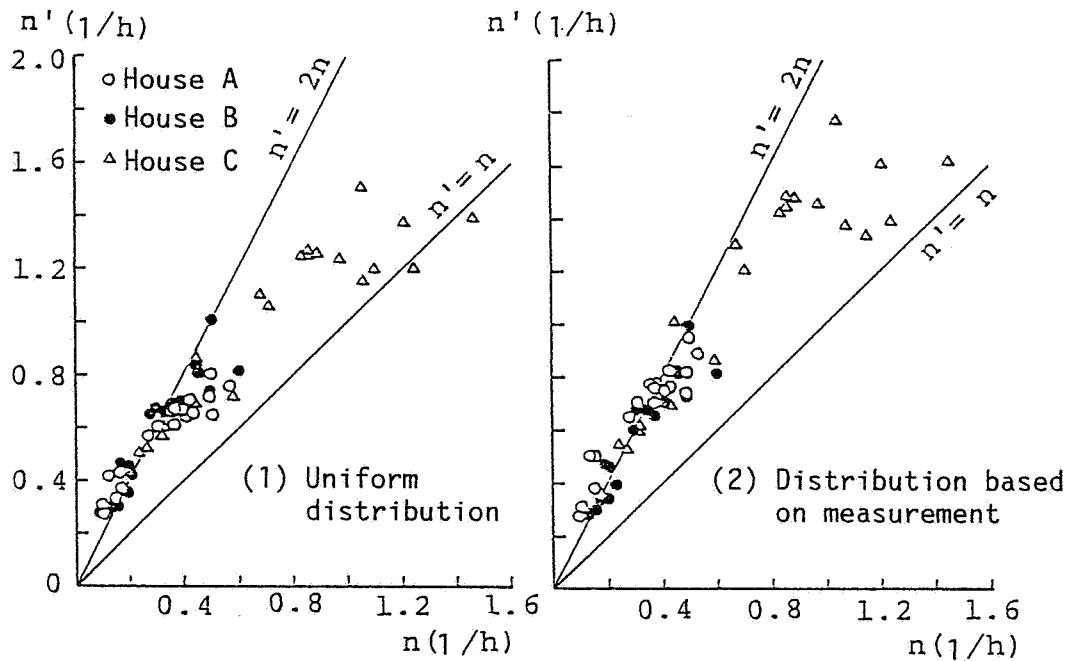


Fig.9 Relationship of infiltration ratios between measurement and calculation with LBL model

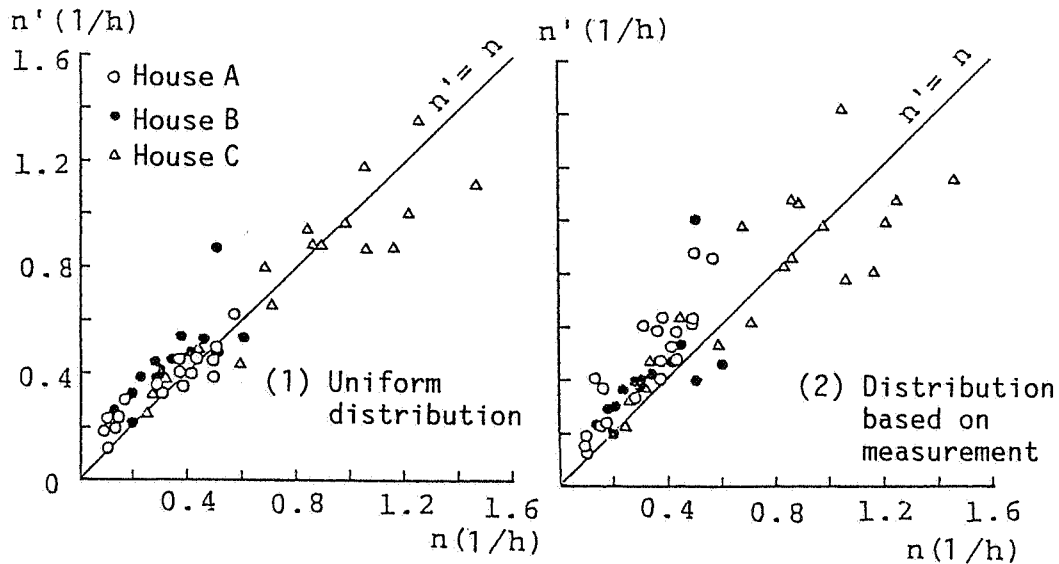


Fig.10 Relationship of infiltration ratios between measurement and calculation with BRE model

3.1.2 Calculated result

Fig.9 shows the relationship between the predicted values and the measured values. The coefficient C' is given by

$$C' = 1/2 (\sqrt{|a_i|}) \quad \text{----- (15)}$$

where a_i is estimated using the measured pressures of House A based on the pressure distribution as shown in Fig.8. Fig.9-(1) is an example of leakage uniformly distributed over the building envelope, while Fig.9-(2) is an example of the leakage uniformly distributed on each wall, ceiling and floor.

The calculated infiltration rates are overestimated in both cases. The predicted values of Houses A and B are twice the measured values, while those of House C are one to two times the measured values. This is probably because with the LBL model infiltration rate is calculated under the assumption that the wind effect and the stack effect act independently, when in fact, these two different effects are often related.

3.2 BRE Model

3.2.1 Model

The values Q_0 and n are calculated by means of Eq.(1) using the result of the pressurization test. The indoor-outdoor pressure difference, Δp_j , acting on the wall i at a height above the floor of Z is given by Eq.(16) which combines the wind and stack effects.

$$\Delta p_j = \rho v^2 (a_i - BZ)/2 \quad \text{----- (16)}$$

where

$$\begin{aligned} a_i &= C_i - C_r \\ B &= 2 T_g H / (T + 273) = 2 A_r \\ Z &= h/H \end{aligned} \quad \text{----- (17)}$$

Under the assumption that leakage is uniformly distributed on each wall, the air flow rate, ΔQ_j , through the part j of wall i is given by

$$dQ_j = (dh/H) Q_{0i} (|\Delta p_j|/\Delta p_0)^n \text{sign}(\Delta p_j) \text{----- (18)}$$

After Eq.(16) is incorporated into Eq.(18), the air flow rate, Q_i , can be obtained by integrating Eq.(18) by Z between 0 and 1. The flow rates through the ceiling and the floor are obtained in the same manner. The indoor pressure, C , is determined by the iterative calculation method using the following equation.

$$\Sigma Q_i + Q_c + Q_f = 0 \quad \text{----- (19)}$$

Consequently, the air infiltration rate is expressed as

$$Q = Q_o (\rho v^2 \Delta p_o / 2)^{1/n} F(A_r, \phi) \quad \text{----- (20)}$$

where,

$$F(A_r, \phi) = [1 / \{2B(1/n+1)\}] \Sigma \{ (Q_i/Q_o) \{ (|a_i|)^{1/n} \text{sign}(a_i) - (|a_i-B|)^{1/n} \text{sign}(a_i-B) \} \} + (Q_f/Q_o) (|a_i|)^{1/n} + (Q_c/Q_o) (|a_c-B|)^{1/n} \quad (21)$$

If the wind effect or the stack effect acts independently, the infiltration rate can be determined by an equation similar to Eq.(21), after slight modification of Eq.(15).

3.2.2 Calculated results

Fig.10-(1) shows the results in the case of uniform leakage distribution over the envelope, while Fig.10-(2) shows results for the case of uniform distribution on each wall. The predicted values of Houses A and B are slightly overestimated, one to two times the measured values. The predicted values of House C are plotted in the range from 0.8 to 1.5 times the measured values. The predicted result for House C under the assumption of uniform distribution, yields a good estimation.

3.3 JCV model

3.3.1 Method of Calculating air infiltration

The indoor-outdoor pressure difference through leakage j at a height h above the floor is expressed by Eq.(22), which combines the wind effect and the stack effect.

$$\Delta p_j = C_j \frac{\rho}{2} v^2 - p_r + h_j (\rho_r - \rho_o) \quad \text{----- (22)}$$

The air flow rate, Q_j , through leakage j is determined by

$$Q_j = Q_{oj} (\Delta p_j)^{1/n_j} \quad \text{----- (23)}$$

Eq.(22) is introduced into Eq.(23), and then Q_j is introduced into Eq.(24). Consequently, the total infiltration rate or air exfiltration rate is equal to zero.

$$\Sigma Q_j = 0 \quad \text{----- (24)}$$

The indoor pressure and the air flow rate of each leakage can be obtained by means of Eq.(24) using the Newton-Raphson iterative calculation method.

Although Eq.(16) and Eq.(22) are expressed differently, they yield the same result.

3.3.2 Leakage distributions for calculation

Air infiltration was calculated under the assumption of there being five types of leakage distributions as shown in Table 5 as estimated by the fan pressurization test. No.1 to No.3 are cases in which leakage characteristics of each building element as shown in Table 1 are used for calculation. However, in the cases of No.2 and No.3, the flow exponent, n , for each element is assumed to be equal to the value obtained by the fan pressurization test for a whole house. This is because the flow exponent of each leakage, as shown in Table 1, is scattered.

The other leakage is assumed to be uniformly distributed over the envelope in the cases of No.1 and No.2, and is also uniformly distributed along the interfaces between the ceiling and the walls and between the walls. In the case of No.4, the leakage is uniformly distributed over the building envelope only. In the case of No.5, the leakage is concentrated at the entrance and the window.

The longitudinal leakage and the uniformly distributed leakage are divided into ten parts. It is assumed that the divided leakage is concentrated at the center of each part. In House C, there is no leakage through the floor because the floor is constructed on a concrete slab which is directly on the ground.

The neutral level of the house having varied leakage distribution can be calculated as shown in Table 6. No.4 is similar to the measured value.

3.3.3 Comparison between calculation and measurement

Fig.11 shows the relationship between the predicted values and the measured values. Table 7 indicates the standard deviation of errors of the predicted values from the measured values divided by the mean of the measured values. This table includes the results calculated by means of the LBL model and the BRE model.

The values predicted under the condition of different leakage distributions differ greatly. But the predicted infiltration rates under the leakage distributions of No.1, No.2 and No.3 have almost equal values, because these three leakage distributions are similar. The scattering of the predicted values under distribution No.4 is smallest, while that calculated under distribution No.5 is largest.

In the case of House A, all of the predicted values overestimate

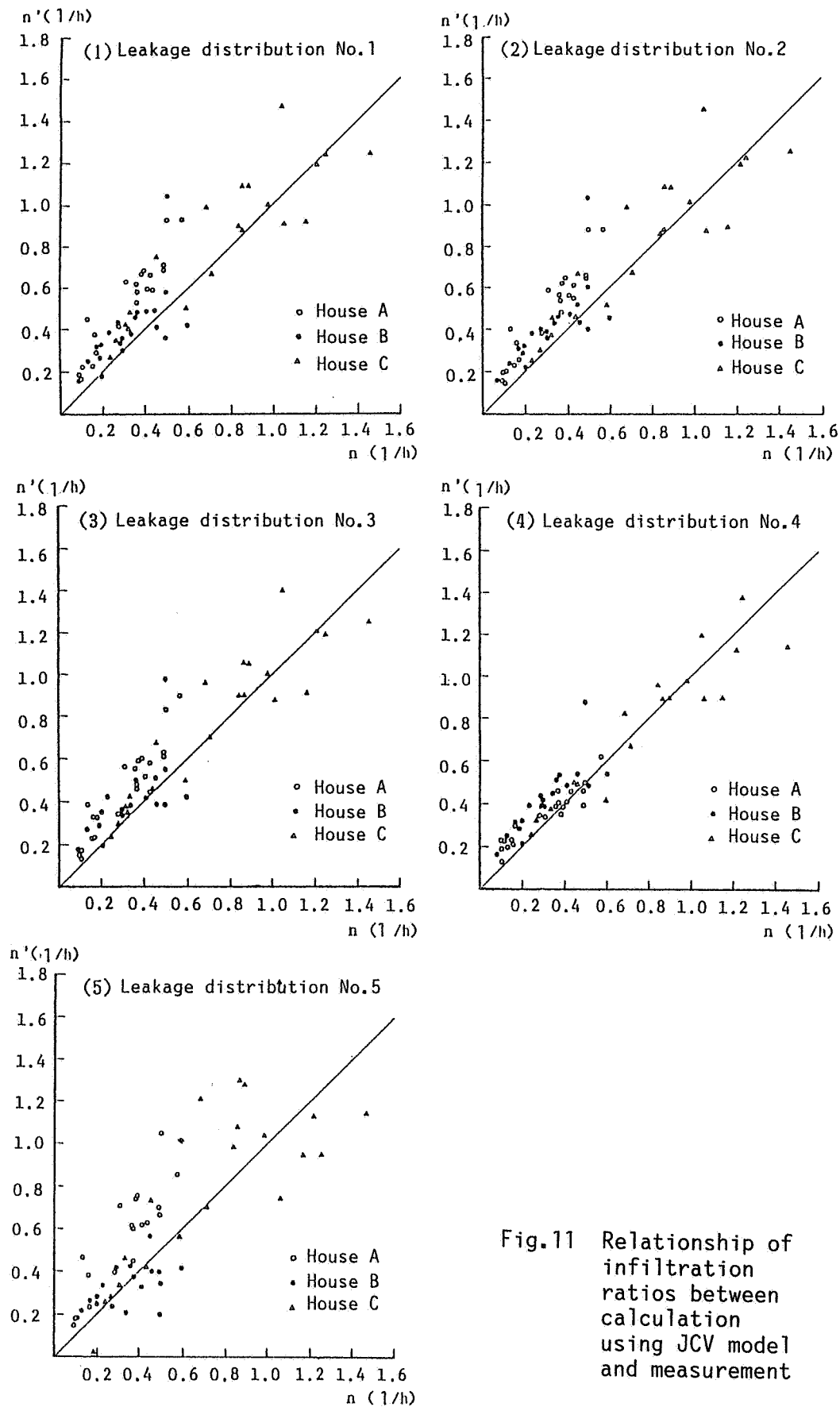


Fig.11 Relationship of infiltration ratios between calculation using JCV model and measurement

Table 5 Leakage distribution and contents

Variation	Contents
No.1	Leakage of each building element is distributed according to the measured result(Table 1).Other obscure leakages are uniformly distributed over the envelope.
No.2	Same as No.1 but the flow component n at each building element is equal to that for a whole house.
No.3	Same as No.2 but other obscure leaks are uniformly distributed along ceiling/wall and wall/wall interfaces.
No.4	The total leakage is distributed over the envelope(House C has no leakage in the floor).
No.5	Total leakage is concentrated at the entrance and the windows.

Table 6 Variation of distribution and height of neutral level (height above the floor : m)

		House A	House B	House C
Measured height of neutral level		1.21	1.30	1.69
Leakage distribution	No. 1	1.42	0.72	1.67
	No. 2	1.42	0.72	1.67
	No. 3	1.42	0.72	1.67
	No. 4	1.22	1.22	1.71
	No. 5	1.37	1.04	1.43

Table 7 The ratio of the standard deviation of error to the average of measured values

Variation of calculation	Variation of leakage distribution	House A	House B	House C
LBL model	Uniform distribution	0.795	0.907	0.391
	Measurement	1.116	0.918	0.568
BRE model	Uniform distribution	0.223	0.416	0.167
	Measurement	0.581	0.470	0.243
JCV model	No. 1	0.745	0.484	0.230
	No. 2	0.622	0.467	0.215
	No. 3	0.539	0.454	0.203
	No. 4	0.223	0.418	0.165
	No. 5	0.802	0.380	0.370

the measured values. Among the three houses, the degree of error from the measured values is greatest for House A except for distribution No.4. In the case of House B, almost all of the predicted values also overestimate the measured values except for distribution No.5. In the case of House C, the calculated results give relatively good estimations under all five distributions. This is probably because the leakage area of House C is great and the leaks are distributed over the envelope.

The reason that uniform distribution No.4 gives a good estimation for all three houses, is that the obscure leaks other than the leaks found around the windows and the entrance make up 36%, 69% and 31% of the total leakage of House A, B and C, respectively; these leaks play an important role in air infiltration by connecting the outdoors and indoors.

The result obtained by distribution No.4 is the same as the result of the BRE model, assuming uniform distribution over the envelope. The difference between the two methods is either due to integration of the air flow along the longitudinal leak or summation of the air flow through the divided leaks.

4. CONCLUSIONS

Calculation models of air infiltration in a single room were verified by measuring the airtightness and the air infiltration in three test houses. The results can be summarized as follows:

- 1) While the ratio of the total leakage of House A, B and C was 1:1.1:1.9, the relation of the mean air infiltration ratio of the three houses was 1:1:2.5. Therefore, the infiltration ratio is not proportionate to the total leakage.
- 2) The air infiltration ratio was expressed by the indoor-outdoor temperature difference and the wind velocity using the linear equation by Bahnfleth, et al. The correlation coefficient between the predicted values obtained by this equation and the measured values was more than 0.9.
- 3) The predicted values found with the LBL model were two times the measured values in the cases of House A and B, and one to two times in the case of House C. This overestimation is probably due to the calculation method under the assumption that the wind effect and the stack effect act independently.
- 4) The predicted values found with the BRE model were one to two times the measured values. However, the calculation for House C under conditions of uniform distribution over the envelope gave a good estimation.
- 5) The accuracy of prediction of the calculation method widely used in Japan, was investigated as to the effects of five types of leakage distributions assumed on the basis of the fan

pressurization test. It was found that the assumption of uniform distribution over the envelope gave the best estimation. This was as expected because the obscure leaks played an important role in air infiltration by connecting the indoors and outdoors.

Therefore, it can be said that in the case of a wooden house which is not particularly airtight, air infiltration can be estimated by the usual calculation method based on the result of the airtightness test for a whole house without measuring the airtightness of every building element.

5. REFERENCES

1. M.H. Sherman and D.T. Grimsrud, "Measurement of Infiltration Using Fan Pressurization and Weather Data", 1st AIC Conference Proceedings, 1982, pp 279-332.
2. P.R. Warren and B.C. Webb, "The Relationship between Tracer Gas and Pressurization Techniques in Dwellings", 1st AIC Conference Proceedings, 1980, pp 245-276.
3. K. Watanabe, "Principle of Architecture Planning Design", Morikita-Shuppan Co., 1951 (in Japanese).
4. S. Murakami and H. Yoshino, "Air-Tightness of Residential Buildings in Japan", 4th AIC Conference Proceedings, 1983, pp 15.1-15.20.
5. D.R. Bahnfleth, T.D. Moseley and W.S Harris, "Measurement of Infiltration in Two Residences, Part II: Comparison of Variables Affecting Infiltration", ASHRAE Transactions, Vol.63, 1957.
6. H. Yoshino, F. Hasegawa and Y. Utsumi, "Evaluation Test of Calculation Method for Air Infiltration Using Test Houses", (Submitted to Transactions on Environmental Engineering in Architecture).